ACS OMEGA

http://pubs.acs.org/journal/acsodf

Article

Compressibility of Abnormal Pressure Gas Reservoirs and Its Effect on Reserves

Jianzhong Zhang and Tianrun Gao*

Cite This: *ACS Omega* 2021, 6, 26221−26230

Read Online

ACCESS | Metrics & More | Article Recommendations

ABSTRACT: The compressibility of abnormal pressure gas reservoirs is hard to test, and the interpretation is confusing, leading to many misunderstandings in the current understanding of abnormal pressure gas reservoirs. In this research, a high-pressure experimental system was designed, and a series of high-pressure compressibility tests of pure water, nitrogen, and rocks under different water saturations were carried out. Then, the effective compressibility of gas reservoirs was calculated; the effect of water saturation on abnormal pressure gas reservoirs and the dynamic prediction was studied. The results show that the compressibilities of water and rock are effectively constant values over the range examined, while the compressibility of gas decreases exponentially with the increase in pressure. The effective compressibility of the stratum increases with the rise of water saturation. The theory of stress and strain of rock mechanics also shows that the rock compressibility is determined by Young's modulus, Poisson's ratio, and porosity and has no connection with the formation pressure. With the increase in water saturation, the swelling degree of the production indicator curve of the simulation experiment becomes larger and larger. After introducing the effective compressibility of the stratum into the gas−water material balance equation, the gas reserves predicted by the revised production indicator curve are the same as the original reserves. The research results have important guiding significance for the efficient development of gas reservoirs.

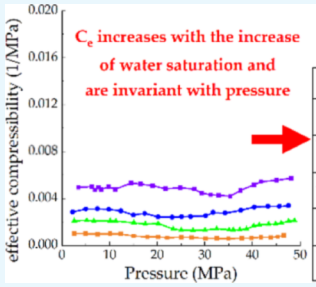

After considering C_e, the prediction deviation of geological reserves is significantly reduced

Water saturation/%	0	38.6	55.5	69.7
Original core reserve/mL	89730.3	55791.9	41515	29429.3
Reserve before correction/mL	89730.3	63892	48904.3	37086.6
Reserve after correction/mL	89730.3	56917.8	42628	30386.3
Deviation before correction/%	0	14.52	17.8	26.02
Deviation after correction/%	0	2.02	2.68	3.25

1. INTRODUCTION

High-pressure (pressure coefficient between 1.3 and 1.8) and ultra-high-pressure (pressure coefficient greater than 1.8) gas reservoirs are distributed worldwide, with burial depths ranging from several hundred meters to several kilometers.[1] There has been rapid growth in the exploration and development of high-pressure and ultra-high-pressure gas reservoirs in China since 2000. At the end of 2020, China has cumulatively proved a total of 2.6×10^{12} m^3 of natural gas reserves in ultra-deep gas reservoirs (burial depth greater than 4500 m), and annual gas production is exceeding 3.0×10^{10} m^3.[2] The Kela 2 gas field in the Tarim Basin and the Longwangmiao Formation gas reservoir in the Sichuan Basin are the two most typical abnormal ultra-high-pressure gas reservoirs in China. The Kela 2 gas field is the primary gas source of China's West-East Gas Pipeline, and its cumulative gas production has exceeded 1.0×10^{11} m^3. The formation pressure corresponding to the Kela 2 gas field is 74.6 MPa, and the pressure coefficient is 2.02.[3] The Longwangmiao Formation gas reservoir is one of the vital gas reservoirs in the central Sichuan oil and gas area, and the proven geological reserves are more than 4.4×10^{11} m^3. The corresponding reservoir pressure and pressure coefficient of Longwangmiao Formation gas reservoir are 75 MPa and 1.7, respectively.[4,5] Ultra-deep gas fields have become the most crucial part of natural gas reserves and production and profit growth. Therefore, a correct understanding of abnormal pressure gas reservoirs' characteristics of geology and development has important guiding significance for gas fields' rational and practical development.

According to the test results of gas *PVT* characteristics, all gas reservoirs can be divided into the low-pressure gas reservoirs (p < 14 MPa), medium-pressure gas reservoirs (14 MPa < p < 21 MPa), and high-pressure gas reservoirs (p > 21 MPa).[1] Furthermore, according to gas reservoirs' net water pressure coefficient, it can be divided into abnormal high-pressure gas reservoirs (pressure coefficient greater than 1.3) and abnormal low-pressure gas reservoirs (pressure coefficient less than 0.8). Actually, there is no essential difference between abnormal pressure gas reservoirs and normal pressure gas reservoirs. It is just that at the same depth, the formation pressure is higher or lower, and the pressure coefficient is only artificially defined and has no physical meaning. Generally, gas

Received: June 21, 2021
Accepted: September 16, 2021
Published: September 28, 2021

reservoirs with a pressure exceeding 30 MPa are regarded as high-pressure gas reservoirs in the actual gas field development process. The higher the reservoir pressure, the higher the reserves, and the greater the development potential. There is no essential difference in development characteristics between abnormal pressure gas reservoirs and normal pressure gas reservoirs. Under the same conditions, due to higher energy, the initial production of abnormal pressure gas reservoirs will be greater. However, for a long time in the past, researchers who have specialized in abnormal pressure gas reservoirs have concluded that development characteristic curves are entirely different from normal pressure gas reservoirs. That is, the production indicator curve of the normal pressure gas reservoir is a straight line,[6] while the production indicator curve of the abnormal pressure gas reservoir is a downward bending line.[7,8] Based on this, it is commonly accepted that the rock compressibility of abnormal pressure gas reservoirs is much higher than that of normal pressure gas reservoirs and will gradually decrease with the depressurization and development of gas reservoirs. Some scientists consider that the rock compressibility of abnormal pressure gas reservoirs is related to the buried depth of the gas reservoir.[9] For example, Chen (2020)[10] established an empirical formula for burial depth and the compressibility of rock and calculated that when the reservoir is buried at 3757 m, the rock compressibility can reach 3.02×10^{-3}/MPa. However, according to the theory of stress and strain of rock mechanics, the rock strain curve is a straight line within the linear elastic range. Therefore, the compressibility of the rock should be constant. When the stress value increases beyond the elastic limit, plastic deformation will occur, and the compression coefficient will increase. Therefore, the above viewpoint is not valid, and it is a misunderstanding of the mechanical behavior of rock.

Due to the high requirements and difficulty in testing the compressibility of the reservoir rock in abnormal pressure gas reservoirs, the experimental test results of the rock compressibility under abnormal pressure were not reported,[11−13] and this perhaps the reason for the misunderstanding of abnormal pressure gas reservoirs.[14,15] This research aims to accurately determine the rock compressibility and correctly understand the development characteristics of abnormal pressure gas reservoirs. In this research, a series of experiments for developing abnormal pressure gas reservoirs were designed to accurately obtain the compressibility of formation rocks under abnormal pressure conditions. First, the compressibility of water and gas was measured under rigid conditions. Then, the comprehensive compressibility of the core under different water saturations was measured, and compressibility of rock was calculated according to the separation method. The results demonstrate that the rock compressibility is a constant in the linear elastic range. Then, considering the effective compressibility of the water-bearing reservoir, the production indicator curve of the abnormal pressure gas reservoir simulation experiment was redrawn, and the reserves and production performance of the abnormal pressure gas reservoir were accurately predicted.

2. EXPERIMENTAL SAMPLES AND METHODS

2.1. Experimental Samples. The core sample used in this experiment is an outcrop core with sandstone properties, and the basic properties are shown in Table 1. The saturated gas is 99.99% pure nitrogen, and the simulated formation water used in the experiment is standard brine with a concentration of 60,000 ppm.

Table 1. Based Properties of Sandstone Cores

length (mm)	diameter (mm)	pore volume (mL)	porosity (%)	gas permeability (mD)
199.09	99.81	244.99	15.73	2.897

2.2. Experimental Methods. The experimental systems were composed of the pressurization system, the core testing system, and the data acquisition system. A flow chart of the experiment is illustrated in Figure 1. First, the high-pressure natural depletion simulation experiments were carried out in the core under the conditions of pure gas (0% water) and pure water (100% water). Then, the simulation experiment of natural depletion of high-pressure gas reservoirs with different water saturations was carried out.

Before carrying out the core natural depletion experiment, the high-pressure (50 MPa) compressibility test of nitrogen and water in a rigid intermediate container was carried out. The purpose is to obtain the compressibility curves of pure water and nitrogen under high pressure to provide a basis for comparison in subsequent core experiments. Detailed experimental procedures are shown in the Appendix.

3. RESULTS AND DISCUSSION

3.1. Compressibility of Water and Gas under Rigid Conditions. The compressibility of water under rigid conditions is defined as the volume change for each unit of pressure increase under the assumption that the system is kept at a constant temperature, which is

$$C_w = -\frac{1}{V_w}\left(\frac{\partial V_w}{\partial p}\right)_T \quad (1)$$

where C_w is the compressibility of water and V_w is the volume of water.

The equation of the compressibility of gas in the rigid state is the relationship between pressure change and unit volume change under the assumption that the system is kept at a constant temperature.[16]

$$C_g = -\frac{1}{V_g}\left(\frac{\partial V_g}{\partial p}\right)_T \quad (2)$$

where C_g is the compressibility of gas and V_g is the volume of gas.

To accurately test the compressibility of rock under high pressure, the compressibility of gas and water was first obtained through the state changes in gas and water in a high-pressure rigid intermediate container. Then, the compressibility of pure rock in water and gas state is calculated using the separation method. The change curve of the compressibility of pure water under high pressure during the depressurization process is shown in Figure 2. From Figure 2, it is clear that the compressibility of water during the entire pressure drop process is basically a constant value (4.3×10^{-4}/MPa). The change curve of the compressibility of pure nitrogen under high pressure during the depressurization process is shown in Figure 3. As can be seen from Figure 3, the compressibility of nitrogen gradually decreases with increasing pressure. In the pressure range of 0−10 MPa, the

https://doi.org/10.1021/acsomega.1c03228
ACS Omega 2021, 6, 26221−26230

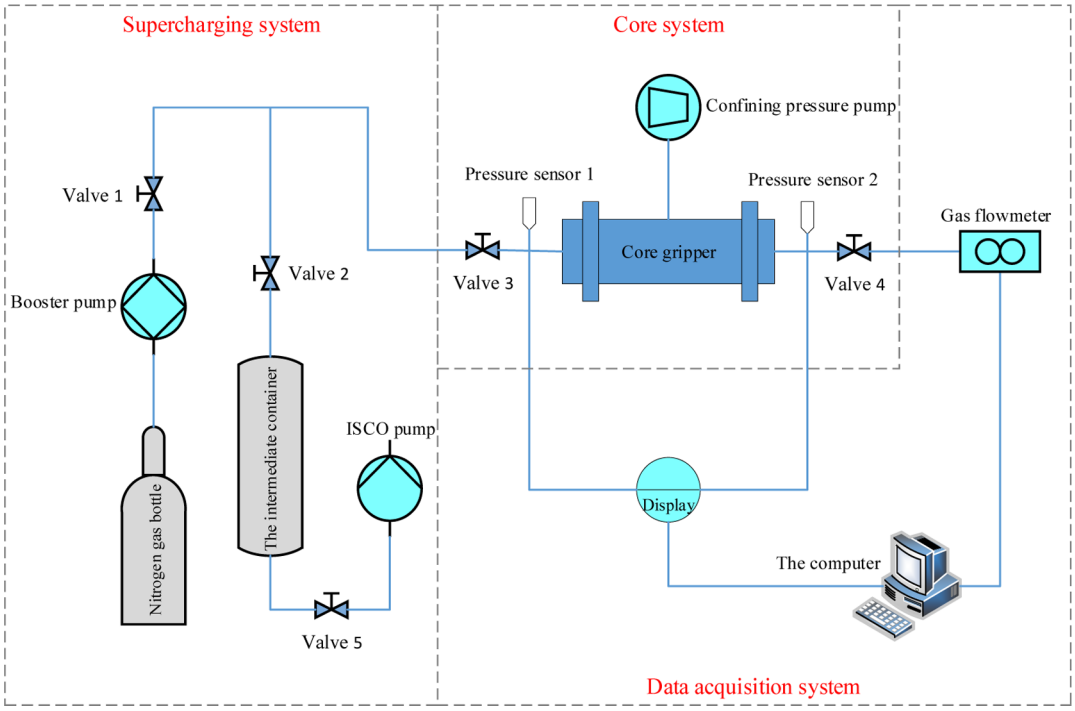

Figure 1. Experimental flow chart of the depletion developments.

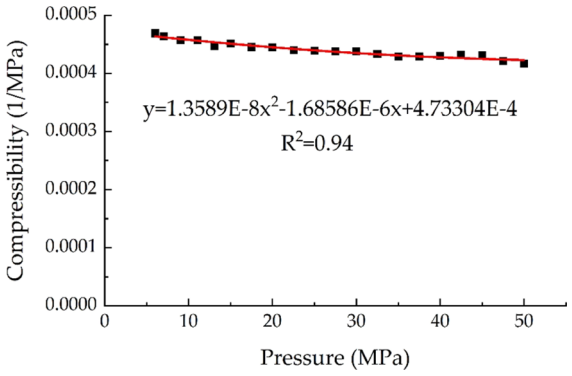

Figure 2. Relationship between water compressibility and pressure.

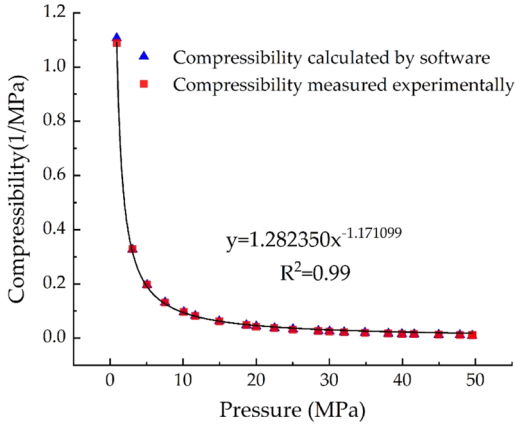

Figure 3. Relationship between the compressibility of nitrogen and pressure.

compressibility of nitrogen varies significantly with the increase in pressure. However, when the pressure is greater than 10 MPa, the level of these changes is relatively small. The compressibility of nitrogen is generally less than 0.1/MPa at formation pressure.

In general, the compressibility of nitrogen changes significantly, especially under high-pressure conditions. The compressibility of gas will also drop to a shallow level. The corresponding compressibility at 50 MPa is about 1.0×10^{-2}/MPa. The higher the pressure, the closer the compressibility of gas gets to that of water.

Under constant temperature conditions, the following expression can be obtained for the actual gas state equation concerning the pressure differential.

$$\frac{dV}{dp} = \frac{nRT}{p}\frac{dz}{dp} - \frac{znRT}{p^2} \tag{3}$$

Substituting the frequently used expression of the compressibility of gas given by eq 2 into the equation above and simplifying it, we get

$$C_g = \frac{1}{p} - \frac{1}{z}\cdot\frac{dz}{dp} \tag{4}$$

To validate the reliability and accuracy of experimental results, the compressibility of nitrogen through the REFPROP[17] software combined with the numerical value of eq 4 is calculated. The experimental measurements showed an agreement with the calculated results predicted by the theory. By fitting and calculating the experimental curve, as shown in Figures 2 and 3, the empirical formula for calculating the compressibility of water and nitrogen can be obtained separately. The empirical formula for curve fitting are

$$C_w = 1.36 \times 10^{-8}p^2 - 1.69 \times 10^{-6}p + 4.73 \times 10^{-4}$$

$$C_g = 1.28p^{-1.17}$$

Based on the reliable primary experimental data and nearly identical fitting results, the compressibility fitting equations of

https://doi.org/10.1021/acsomega.1c03228
ACS Omega 2021, 6, 26221−26230

pure water and gas under high pressure can be used to perform predictions on the compressibility of gas and water under higher pressure (50−100 MPa) that are difficult to test (Figure 4). According to the fitting results, within the pressure range of

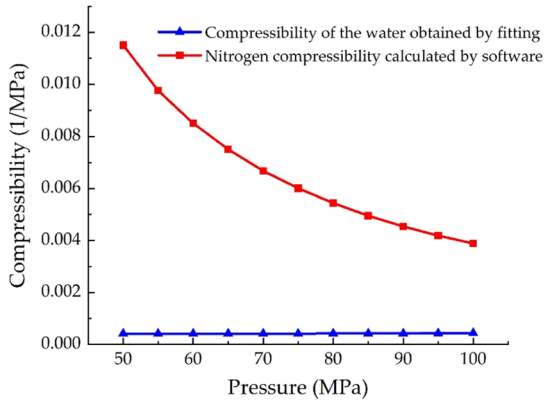

Figure 4. Compressibility of gas and water obtained by fitting at 50−100 MPa.

100 MPa, the compressibility of water changes very little, which can be regarded as a constant value, about $(4.2-4.4) \times 10^{-4}$/MPa. On the other hand, the compressibility of nitrogen will continue to decrease with the pressure increment, and it becomes closer and closer to the compressibility of water. After 90 MPa, the compressibility of gas drops to about 3.9×10^{-3}/MPa, which means that the difference between those two becomes less than an order of magnitude. Thus, it can be found that the influence of the compressibility of water and rock cannot be ignored in the development process of high-pressure (significantly abnormal pressure) gas reservoirs.

3.2. Compressibilities under Experimental Conditions. The compressibility of the rock mentioned in this article is also called the compressibility of pore volume, which is defined as the fractional change in unit pore volume with pressure, namely

$$C_p = \frac{1}{V_p}\frac{\Delta V_p}{\Delta p} \tag{5}$$

where C_p is the compressibility of the rock (the compressibility of pore volume) and V_p is the pore volume of the rock.

When the formation pressure of the gas reservoir decreases, on the one hand, the pore volume shrinks by ΔV_p, and on the other hand, the fluid expands by ΔV_L. These two effects can drive part of the formation fluid from the formation to the production well. For example, in a formation rock with a volume of V_b, when the formation pressure drops by Δp, the gas volume ΔV produced by the combined action of the two is[18]

$$\Delta V = \Delta V_p + \Delta V_L \tag{6}$$

then

$$V_L = V_b \cdot \phi = V_p \tag{7}$$

Substituting eqs 7 into 6, we get

$$\Delta V = C_p V_p \Delta p + C_L V_p \Delta p = V_p \Delta p (C_p + C_L) = V_p \Delta p [C_p + (C_g S_g + C_w S_w)] \tag{8}$$

where C_L is the compressibility of the fluid.

The combined compressibility of the core is defined as the total volume change of pores and fluids in unit pore volume for each unit formation pressure drop, namely

$$C_t = \frac{1}{V_p}\frac{\Delta V}{\Delta p} \tag{9}$$

where C_t is the combined compressibility of the core.

Therefore, when the formation contains gas and water, the mathematical relationship of the combined compressibility of the core is

$$C_t = C_g S_g + C_w S_w + C_p \tag{10}$$

where S_g and S_w are the saturation of gas and water, respectively, and C_g, C_w, and C_p are the compressibilities of gas, water, and rock, respectively.

The compressibilities measured by the core experiment in saturated pure gas and pure water are shown in Figure 5. According to eq 10, the compressibility of rock under soaking water and saturated gas can be obtained, respectively. It can be found that although the value of the compressibility of rock obtained by the two conditions fluctuates with the change in

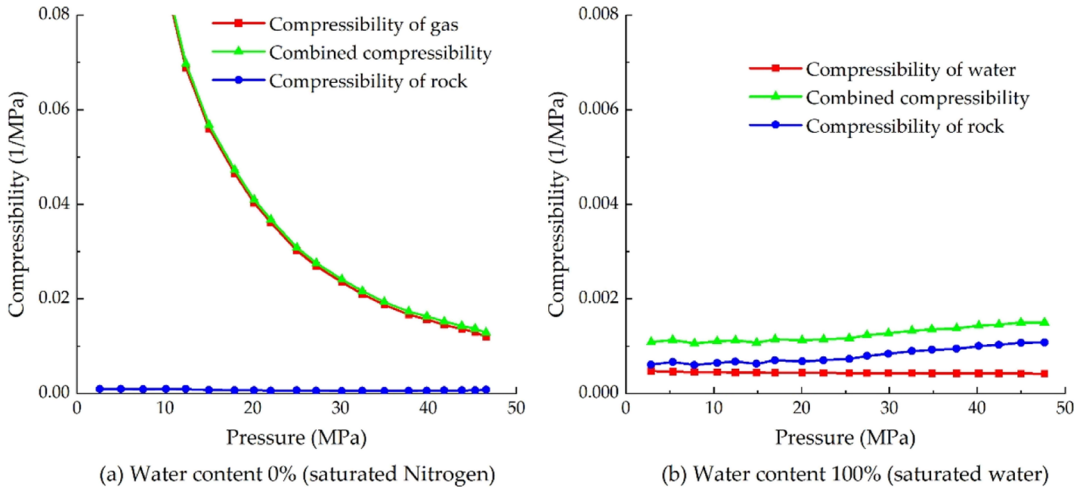

(a) Water content 0% (saturated Nitrogen) (b) Water content 100% (saturated water)

Figure 5. Compressibility tested under saturated pure gas and pure water conditions.

https://doi.org/10.1021/acsomega.1c03228
ACS Omega 2021, 6, 26221−26230

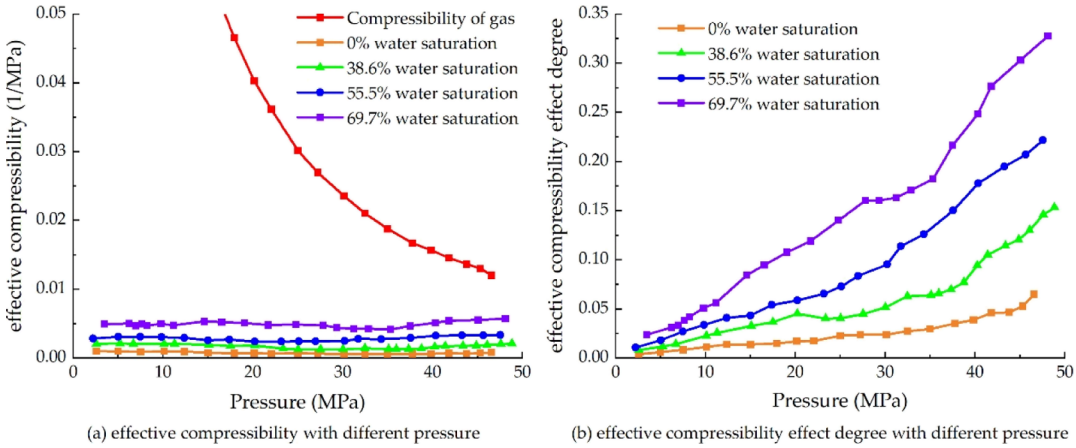

(a) effective compressibility with different pressure (b) effective compressibility effect degree with different pressure

Figure 6. Effective compressibility with different water saturations and their effect degree.

pressure, it is maintained within the range of 6.0×10^{-4}/MPa to 1.0×10^{-3}/MPa. Considering the experimental error, the compressibility of rock can basically be regarded as a constant, about 8.0×10^{-4}/MPa.

The decrease in formation pressure during the depletion development of high-pressure gas reservoirs will cause connate water expansion and pore compression. The result of this change is a decrease in the volume of hydrocarbons in the reservoir. Therefore, the effective compressibility of the stratum C_e can be defined. Its physical meaning is the relative change in natural gas volume caused by reservoir water expansion and rock pore volume compression for every 1 MPa drop in formation pressure. This can be used to calculate the effect of the compressibility of water and rock on gas, and the effective compressibility effect degree can be characterized by the parameter η.

$$C_e = \frac{S_w \cdot C_w + C_f}{1 - S_w} \tag{11}$$

$$\eta = \frac{C_e}{C_e + C_g} \tag{12}$$

where C_e is the effective compressibility of the stratum, C_f is the compressibility of stratum (same as the compressibility of rock), and η is the effective compressibility effect degree.

Figure 6 shows the test, calculation results, and the degree of influence on gas reservoirs of the effective compressibility of the stratum of core natural depletion experiments with different water saturations. It can be seen that under the same water saturation, the effective compressibility of the stratum is constant, independent of pressure changes. Still, the effective compressibility effect degree increases with pressure. At the same pressure, both C_e and η increase with the increase in water saturation. Under the conditions of 45 MPa pressure and 38.6% water saturation, the effective compressibility of the stratum has reached about 2.1×10^{-3}/MPa, and the compressibility of gas is about 1.2×10^{-2}/MPa. The value of the effective compressibility of the stratum has reached 17.5% of the value of the compressibility of gas. The higher the pressure and the higher the water saturation, the smaller the difference between C_e and C_g and the greater the effective compressibility effect degree. Therefore, the relevant engineering calculations in the abnormal pressure gas reservoir development process must consider the effect of the effective compressibility of stratum on gas reserves and production. However, according to the trend of the compressibility of gas and reservoir effective compressibility curve, with the increase in pressure and water saturation, the effective compressibility of the stratum will gradually approach the compressibility of gas (see Figure 6a). The effect degree of effective compressibility on a non-water gas reservoir is small, and it is only about 6% at a high pressure of 50 MPa. In the gas reservoir with a water saturation of 38.6%, η can reach about 15%, and the higher the water saturation, the greater the effect degree of effective compressibility (see Figure 6b). It is further indicated that the effective compressibility of the stratum significantly influences the calculation of gas reserves and production during the early natural depletion process of abnormal pressure gas reservoirs, which cannot be ignored.

It can be seen that there is a deviation from the belief that the high production of abnormal pressure gas reservoirs is because the compressibility of rock is greater than the compressibility of gas.

Table 2 shows the compressibility of rock and the effective compressibility of the stratum with different water saturations within 50 MPa. It can be seen that water saturation has little effect on the compressibility of rock but has a significant effect on the effective compressibility of the stratum of simulated gas reservoirs. The greater water saturation, the greater the effective compressibility of the stratum. It indicates that high water saturation has an evident influence on the gas reservoir development performance.

Table 2. Compressibility with Different Water Saturations

water saturation/%	0	38.6	55.5	69.7
the compressibility of rock/10^{-3}/MPa	0.5−1	0.6−1.2	0.8−1.3	0.9−1.4
the effective compressibility/10^{-3}/MPa	0.5−1	1.2−2.1	2.3−3.4	4.1−5.8

3.3. Case Study of the Influence of the Compressibility of Rock. Figure 7 shows the prediction and actual production results of the annual gas production per unit pressure drop of an abnormal pressure gas reservoir (buried depth of about 4000 m, formation pressure of about 80 MPa, and pressure coefficient of about 2). The project prediction is based on the knowledge that the compressibility of rock of abnormal pressure gas reservoirs is much higher than that of conventional gas reservoirs. Therefore, the gas production per unit pressure drop of the abnormal pressure gas reservoir will

https://doi.org/10.1021/acsomega.1c03228
ACS Omega 2021, 6, 26221−26230

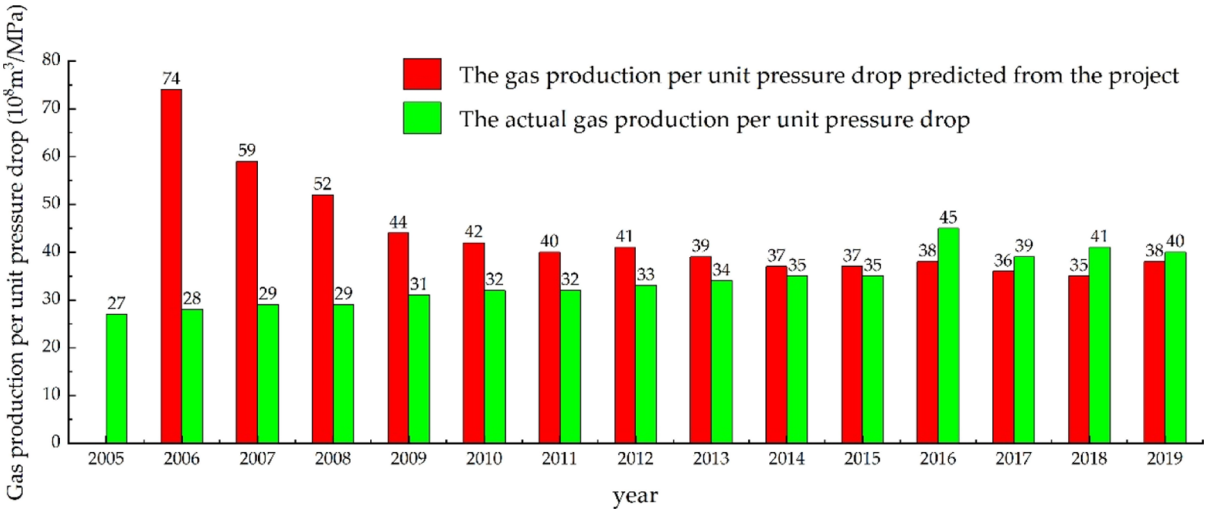

Figure 7. Comparison of annual gas production per unit pressure drop for an abnormal pressure gas reservoir with the design value of the project.

Table 3. Basic Mechanical Parameters of Different Rocks and the Compressibility of the Skeleton

rock type	sandstone	limestone	dolomites	quartzite
Young's modulus/10^4 MPa	1−10	5−10	5−9.4	6−20
Poisson's ratio	0.2−0.3	0.2−0.35	0.15−0.35	0.08−0.25
Skeleton compressibility/10^{-4}/MPa	0.12−1.8	0.09−0.36	0.09−0.42	0.07−0.42

be significantly higher than that of the actual gas reservoir before the pressure predicted by the project drops to the normal pressure (40 MPa). However, the actual production performance of the gas reservoir shows that the annual gas production per unit pressure drop of the gas reservoir in the first eight years is significantly lower than the predicted results of the project. Moreover, with the progress of gas reservoir production, the annual gas production per unit pressure drop of the gas reservoir not only does not decrease but also gradually increases year by year. The replenishment of energy by the edge and bottom water may be the main reason for the slight increase in the gas production per unit pressure drop in the middle and later period of the gas reservoir development.

In general, the annual gas production per unit pressure drop has not changed much during the 14-year production process of the gas reservoir. The development effect of abnormal pressure gas reservoirs proves that it is wrong to believe that the compressibility of rock of the abnormal pressure gas reservoirs is greater than that of the conventional gas reservoirs. The results of gas reservoir development and physical simulation experiment both show that the compressibility of rock is a constant value and irrelevant to the pressure of the gas reservoir.

3.4. Influence of Lithology on the Compressibility. Rock is composed of two parts: skeleton particles and intergranular pores. Therefore, the decrease in pore volume can be considered to be caused by the compression of the rock skeleton. Hence

$$\Delta V_p = \Delta V_s \tag{13}$$

where V_s is the volume of the skeleton.

Therefore, the compressibility of the skeleton can be expressed as

$$C_s = -\frac{1}{V_s}\cdot\frac{\Delta V_s}{\Delta p} = \frac{V_p}{V_s}\cdot\left(-\frac{\Delta V_p}{V_p \Delta p}\right) = \frac{\phi}{1-\phi}\cdot C_p \tag{14}$$

where C_s is the compressibility of the skeleton and ϕ is the porosity.

According to the theory of stress and strain of rock mechanics,[18] under the condition of elastic deformation, the compressibility of the skeleton can be expressed by the following formula

$$C_s = \frac{3(1-2\nu)}{E} \tag{15}$$

where ν is Poisson's ratio of the skeleton and E is Young's modulus of the skeleton.

From the literature,[19] one can obtain Young's modulus and Poisson's ratio of several typical rocks and use eq 15 to calculate the compressibility of the skeleton (see Table 3). Since the core of the simulation experiment is sandstone, according to the theory of stress and strain of rock mechanics, the compressibility of the skeleton of sandstone is $C_s \approx 1.2 \times 10^{-5}$/MPa to 1.8×10^{-4}/MPa. The abovementioned core experimental research results show that the compressibility of rock of the experimental core is $C_p \approx 6.0 \times 10^{-4}$/MPa to 1.0×10^{-3}/MPa. It can be obtained from eq 14 that the compressibility of the skeleton of the experimental core $C_s \approx 9.0 \times 10^{-5}$/MPa to 2.1×10^{-4}/MPa. Thus, it can be seen that the compressibility of the skeleton calculated by both the theory and experimental methods is basically the same, which proves that the experimental results are consistent with rock mechanical behavior, accurate, and reliable.

It can also be seen from Table 3 that the skeleton compressibility of limestone, dolomite, and quartzite is not much different, while the skeleton compressibility of sandstone is significantly greater than that of these three types of rocks. This shows that the compressibility of the skeleton varies with

https://doi.org/10.1021/acsomega.1c03228
ACS Omega 2021, 6, 26221−26230

lithology, not all rocks have the same value, and the final value is determined by Young's modulus and Poisson's ratio of the rock. It can be seen that the compressibility of rock is mainly affected by lithology and porosity. It also shows that under the same conditions, the sandstone gas reservoirs have the most obvious influence on the gas reservoir reserves and production performance prediction in the four lithological gas reservoirs.

3.5. Influence of Water Saturation on Reserve Calculation. The material balance equation is an expression of the law of conservation of mass, which is widely used in the calculation of oil and gas reservoir engineering. For example, for a constant volume and closed gas reservoir, if the compressibility of formation and water is negligible, it can be expressed in the following form under the assumption of no water production.[20]

$$\frac{p}{z} = \frac{p_i}{z_i}\left(1 - \frac{G_p}{G}\right) \tag{16}$$

where p is the gas reservoir pressure during production, z is the deviation factor of gas during production, p_i is the gas reservoir pressure under original condition, z_i is the deviation factor of gas under original condition, G_p is the gas reservoir production (cumulative), and G is the original gas reserves (geological reserves).

It can be seen from eq 16 that under the condition of neglecting the compressibility of formation and water, there is a linear relationship between the apparent pressure $p_p = p/z$ of the gas reservoir and the cumulative gas production G_p of the gas reservoir (see Figure 8). The relationship curve is called

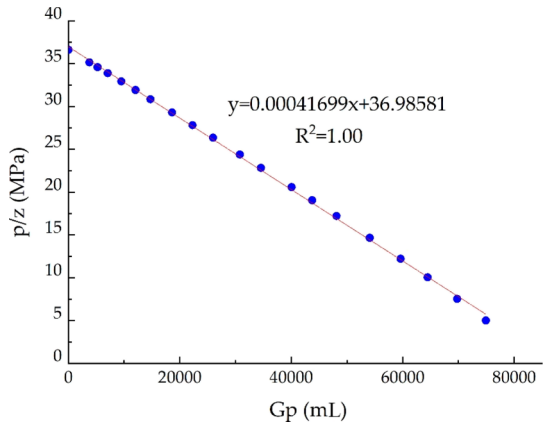

Figure 8. Curve of the relationship between apparent pressure and gas production in a closed dry gas reservoir with constant volume.

the gas reservoir production indicator curve. The intercept of the gas reservoir production indicator curve on the G_p coordinate axis is G, which is the geological reserves of the gas reservoir determined by the gas reservoir's dynamic production data, usually called dynamic geological reserves.

When the compressibility of the formation and water cannot be ignored, the material balance equation under the assumption of no water production can be modified into the following form.[21]

$$\frac{p}{z}(1 - C_e\Delta p) = \frac{p_i}{z_i}\left(1 - \frac{G_p}{G}\right) \tag{17}$$

Figure 8 shows the natural depletion dynamic indicator curve for the 100% gas-saturated core. As shown in Figure 8, the apparent pressure has an excellent linear relationship with the cumulative gas production, which is in full compliance with the material balance equation. When the apparent pressure is 0, the corresponding cumulative gas production is the core geological reserve G. This method can accurately predict the geological reserves of a closed dry gas reservoir with a constant volume.

As shown in Figures 9−11, the left picture is the production indicator curve results of the corresponding natural depletion simulation experiment with the core water saturation of 38.6, 55.5, and 69.7%. It can be found that when the gas reservoir contains water, the production indicator curve is no longer a straight line but an upward convex curve. Therefore, the geological reserves predicted from the production data in the early stage of gas reservoir development will lead to significant errors with the later production performance. The red dotted line in the left figure is the prediction curve of the relationship between apparent pressure and cumulative gas production. Compared to the experimental data points, the predicted dynamic reserves and the corresponding formation apparent pressure results for the same cumulative gas production are obviously larger. The higher the water saturation, the greater the convexity of the curve, and the greater the error of the prediction results. The main reason for this phenomenon is that with the increase in water saturation, the effective compressibility of the stratum increases significantly (see Table 2 and Figure 6), and the gap between this and the compressibility of the gas under the initial high-pressure state of the gas reservoir decreases. The higher the gas reservoir pressure, the smaller the gap between the two, and the more obvious the effect of the effective compressibility of the stratum.

Considering the effective compressibility of the stratum, eq 16 is modified to eq 17, and it can be found that the corrected apparent pressure of the gas reservoir is $p_f = p/z\ (1 - C_e\Delta p)$, which presents a linear relationship with the cumulative gas production G_p. The corrected production indicator curve fits the straight line very well (Figures 9−11 right), and the correlation is high, which can be used to effectively and accurately predict the geological reserves of water-bearing gas reservoirs.

Table 4 lists the original gas reserves of the core, the geological reserves G' and G predicted by the production indicator curve before and after revision, respectively, under different water saturations, and calculates the deviation of geological reserves and original core reserves before and after revision (the ratio of the absolute value of the difference between the predicted reserves and the original reserves to the original reserves of the core). It can be seen that in the production indicator curve before the revision, the deviation between the gas reservoir reserves predicted by the early development data and the actual gas production is large. With the increase in water saturation, the deviation of geological reserves reached 14.52, 17.80, and 26.02%, and the corresponding deviations after correction are 2.02, 2.68, and 3.25%, respectively. The former deviation can be considered to be too large.

It can be seen that in the development process of high-pressure water-bearing gas reservoirs, if the indicator curve fitted to the early production data of the gas reservoir is directly applied without correction, the prediction result of the gas reservoir's geological reserves will be significantly larger, which may easily mislead subsequent production. After

https://doi.org/10.1021/acsomega.1c03228
ACS Omega 2021, 6, 26221−26230

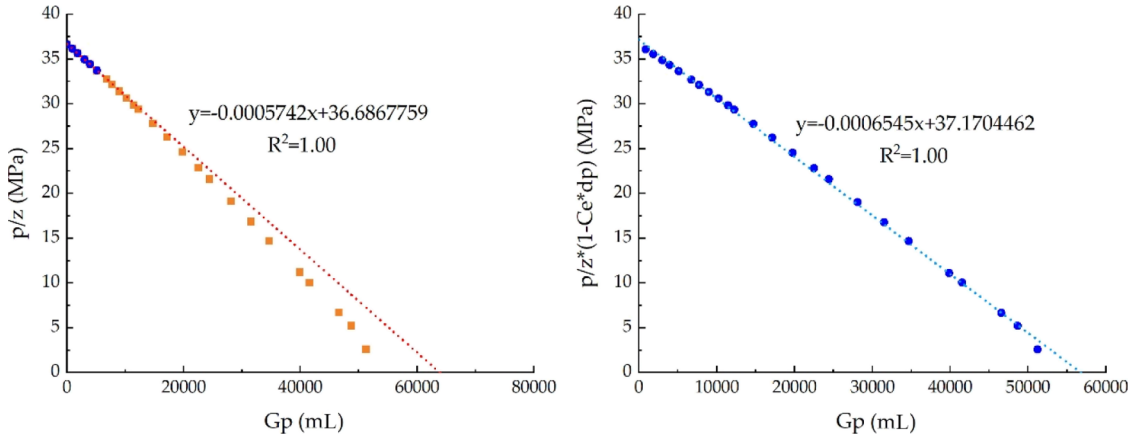

Figure 9. Comparison of production indicator curves before and after correction when core water saturation is 38.6%.

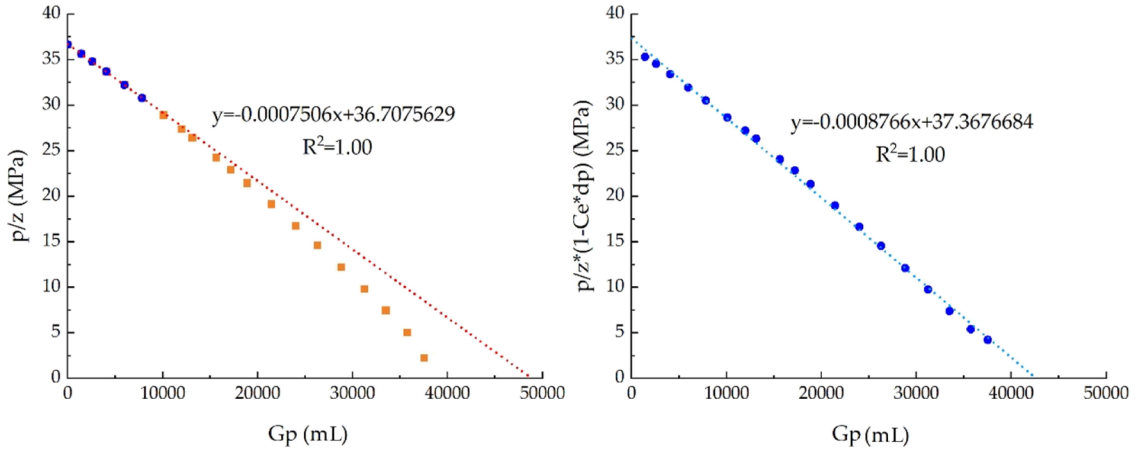

Figure 10. Comparison of production indicator curves before and after correction when core water saturation is 55.5%.

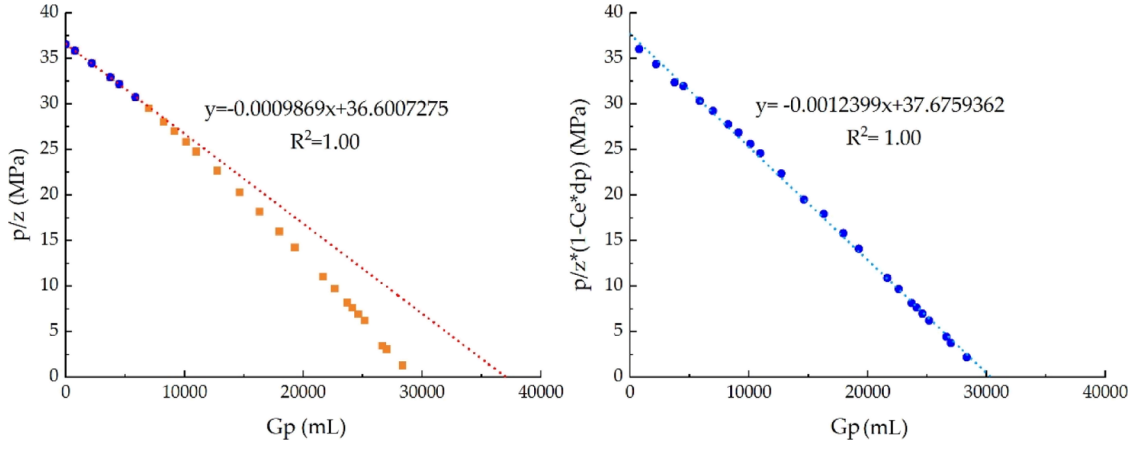

Figure 11. Comparison of production indicator curves before and after correction when core water saturation is 69.7%.

considering the compressibility of the formation and water in the material balance equation (i.e., the effective compressibility of the stratum is introduced in the material balance equation), the difference between the gas geological reserve and the original gas reserve of the core is much smaller than that before correction (within 3.3%).

4. CONCLUSIONS

(1) The compressibility of pure water is basically a constant value, which remains at about 4.3 × 10^{-4}/MPa, and will decrease slightly as the pressure increases. The compressibility of nitrogen rapidly increases with the pressure; after 10 MPa, it will gradually become flat. Under high pressure, the gap between the compressibility of nitrogen and that of water is getting smaller and smaller. The compressibility of rock is a constant value, and the test range is distributed in 6.0 × 10^{-4}/MPa to 1.0 × 10^{-3}/MPa range, slightly larger than the compressibility of water. The effective compressibility of the stratum increases with the increase in water

https://doi.org/10.1021/acsomega.1c03228
ACS Omega 2021, 6, 26221−26230

Table 4. Comparison of Gas Reserves before and after Correction for Different Water Saturations

water saturation/%	0	38.6	55.5	69.7
original core reserve/mL	89,730.3	55,791.9	41,515.0	29,429.3
reserve before correction/mL	89,730.3	63,892.0	48,904.3	37,086.6
reserve after correction/mL	89,730.3	56,917.8	42,628.0	30,386.3
deviation before correction/%	0	14.52	17.80	26.02
deviation after correction/%	0	2.02	2.68	3.25

saturation, and the effective compressibility of the stratum under high water saturation may reach the same order of magnitude as the compressibility of gas under high pressure, which is a factor that cannot be ignored in the material balance equation.

(2) In abnormal pressure gas reservoirs, the compressibility of rock and water are constant values and are invariant with pressure. In contrast, the compressibility of gas will be closer and closer to the compressibility of rock and water under overpressure, and it will reach the same order of magnitude as the effective compressibility of the stratum. Therefore, it is not the change in compressibility of rock that affects the characteristics of the production indicator curve of abnormal pressure gas reservoirs but the increase in the effective compressibility of the stratum for the water-bearing gas reservoir.

(3) According to the theory of stress and strain of rock mechanics, the compressibility of the skeleton varies with lithology and is determined by Young's modulus and Poisson's ratio of the rock. Therefore, the compressibility of rock is mainly affected by its lithology and porosity. The compressibility of the skeleton of sandstone is significantly greater than that of limestone, dolomite, and quartzite.

(4) The production indicator curve of a closed water-bearing gas reservoir with constant volume is not a straight line but an upward convex curve. With the increase in water saturation, the degree of convexity of the curve becomes larger and larger, and the gap between the gas reservoir reserves obtained by fitting the production data at the early stage of development and the dynamic geological reserves becomes larger and larger. After considering the compressibility of the formation and water (i.e., the effective compressibility of the stratum is introduced in the equation), the gas reservoir geological reserves predicted by the revised production indicator curve are consistent with the original geological reserves.

APPENDIX

The detailed process of the experiment is as follows:

(1) The valves 1 and 2 were opened, and a booster pump was used to fill 50 MPa nitrogen into the rigid intermediate container. The valves 1 and 2 were closed, and the valve 5 was opened. An high pressure and high precision plunger (ISCO) pump was used to maintain 50 MPa constant pressure at the bottom of the intermediate container, ready for core saturation high-pressure gas.

(2) The valves 2 and 3 were opened, and the valve 4 was closed. Nitrogen was charged into the core through the constant pressure intermediate container until the pressure at both ends of the core reaches 50 MPa and becomes stable. Then, the valve 3 was closed to prepare for the natural depletion simulation experiment. As pore pressure increases, the ambient pressure also increases until 60 MPa.

(3) The valve 4 was opened, and the simulation experiment of constant flow natural depletion of saturated gas core under high pressure was started. Inlet and outlet pressure sensors 1, 2, and the gas flowmeter were used to continuously record the pressure and outlet flow data until the inlet pressure drops to 0. The combined compressibility of the core with 100% saturated gas was calculated.

(4) Four different water saturations, 100, 69.7, 55.5, and 38.6%, were established, respectively. The combined compressibility of the core under 100% saturated water pressure was first tested. Then, steps 1−3 under the other three different water saturations were repeated to calculate the combined compressibility of the core under different water saturations.

(5) According to the compressibility of pure water and gas, the compressibility of rock and the effective compressibility of the stratum under different water saturations were calculated, respectively.

At the end of all the experiments, the measurement calibration of various dead volumes during the experiment, including the volume of the intermediate container, the volume of both ends of the gripper, the volume of the ISCO pump, the volume of the pipeline, and the volume of each valve, and so forth, was carried out to minimize the experimental errors.

AUTHOR INFORMATION

Corresponding Author

Tianrun Gao − *Tianjin University, Tianjin 300072, China*; Email: gaotianrun1@163.com

Author

Jianzhong Zhang − *University of Chinese Academy of Sciences, Beijing 100049, China*; orcid.org/0000-0003-2506-9349

Complete contact information is available at: https://pubs.acs.org/10.1021/acsomega.1c03228

Notes

The authors declare no competing financial interest.

REFERENCES

(1) Jiang, T.; Sun, X. Development of Keshen ultra-deep and ultra-high pressure gas reservoirs in the Kuqa foreland basin, Tarim Basin: Understanding points and technical countermeasures. *Nat. Gas Ind.* **2018**, *38*, 1−9.

(2) Li, X.; Guo, Z.; Hu, Y.; Luo, R.; Su, Y.; Sun, H.; Liu, X.; Wan, Y.; Zhang, Y.; Li, L. Efficient development strategies for large ultra-deep structural gas fields in China. *Pet. Explor. Dev.* **2018**, *45*, 118−126.

(3) Jia, C.; Zhou, X.; Wang, Z.; Li, Q.; Pi, X.; Cai, Z.; Hu, X. Petroleum geological characteristics of Kela-2 gas field. *Chin. Sci. Bull.* **2002**, *47*, 94−99.

(4) Wei, G.; Du, J.; Xu, C.; Zou, C.; Yang, W.; Shen, P.; Xie, Z.; Zhang, J. Characteristics and accumulation mode of large-scale Sinian-Cambrian gas reservoirs in the Gaoshiti-Moxi region, Sichuan Basin. *Pet. Res.* **2016**, *1*, 164−177.

(5) Wu, J.; Liu, S.; Wang, G.; Zhao, Y.; Sun, W.; Song, J.; Tian, Y. Multi-stage hydrocarbon accumulation and formation pressure evolution in Sinian-Dengying Formation-Cambrian Longwangmiao

Formation, Gaoshiti-Moxi structure, Sichuan Basin. *J. Earth Sci.* **2016**, *27*, 835−845.
(6) Havlena, D.; Odeh, A. S. The material balance as an equation of a straight line. *J. Pet. Technol.* **1963**, *15*, 896−900.
(7) Hammerlindl, D. J. Predicting Gas Reserves in Abnormally Pressured Reservoirs. *Fall Meeting of the Society of Petroleum Engineers of AIME, Paper SPE-3479-MS, New Orleans, Louisiana, USA, October 3−6, 1971*, 1971.
(8) Duggan, J. O. The Anderson "L"—An abnormally pressured gas reservoir in South Texas. *J. Pet. Technol.* **1972**, *24*, 132−138.
(9) Adel, M. E. Analytical and Numerical Solutions for Estimating the Gas In-Place for Abnormal Pressure. *International Meeting on Petroleum Engineering, Paper SPE 29934-MS, Beijing, China, November 14−17, 1995*, 1995.
(10) Chen, Y. Q. *Modern Petroleum Reservoir Engineering*, 2nd ed.; Petroleum Industry Press: Beijing, 2020; pp 69−71.
(11) Dadmohammadi, Y.; Misra, S.; Sondergeld, C.; Rai, C. Petrophysical interpretation of laboratory pressure-step-decay measurements on ultra-tight rock samples. Part 2-In the presence of gas slippage, transitional flow, and diffusion mechanisms. *J. Pet. Sci. Eng.* **2017**, *158*, 554−569.
(12) Macini, P.; Ezio, M.; Salomoni, V. A.; Schrefler, B. A. Casing influence while measuring in situ reservoir compaction. *J. Pet. Sci. Eng.* **2006**, *50*, 40−54.
(13) Jalalh, A. A. Compressibility of porous rocks: Part I. Measurements of Hungarian reservoir rock samples. *Acta Geophys.* **2006**, *54*, 319−332.
(14) El-Ahmady, M. H.; Wattenbarger, R. A.; Pham, T. T. Overestimation of Original Gas in Place in Water-Drive Gas Reservoirs Due to a Misleading Linear p/z Plot. *J. Can. Pet. Technol.* **2002**, *41*, 38−43.
(15) He, J.; Ling, K.; Pei, P.; Ni, X. Calculation of rock compressibility by using the characteristics of downstream pressure change in permeability experiment. *J. Pet. Sci. Eng.* **2016**, *143*, 121−127.
(16) Poston, S. W.; Berg, R. R. *Overpressured Gas Reservoirs*; Petroleum Industry Press: Beijing, 2003.
(17) Lemmon, E. W.; Huber, M. L.; Mclinden, M. O. *REFPROP 9.1. NIST Standard Reference Database 23*; National Institute of Standards and Technology: Boulder, 2013.
(18) Tiab, D.; Donaldson, E. C. *Petrophysics*, 2nd ed.; Gulf Professional Publishing: Houston, 2003.
(19) *Structural Geology*, 2nd ed.; Xie, R. H., Qu, T. X., Qian, G. M., Eds.; China University of Mining and Technology Press: Xuzhou, 2007.
(20) Ramagost, B. P.; Farshad, F. F. P/Z abnormally pressured gas reservoirs. *SPE Annual Technical Conference and Exhibition, Paper SPE-10125-MS, San Antonio, Texas, USA, October 4−7, 1981*, 1981.
(21) Gonzales, F. E.; Ilk, D.; Blasingame, T. A. A quadratic cumulative production model for the material balance of an abnormally pressured gas reservoir *SPE Western Regional/AAPG Pacific Section Joint Meeting, Paper SPE 114044-MS, Bakersfield, California, USA, March 29−April 2, 2008*, 2008.

https://doi.org/10.1021/acsomega.1c03228
ACS Omega 2021, 6, 26221−26230